



Quantitation of class IA PI3Ks in mice reveals p110-free-p85s and isoform-selective subunit associations and recruitment to receptors

N. Tsolakos^{a,1}, T. N. Durrant^{b,1}, T. Chessa^{a,1}, S. M. Suire^a, D. Oxley^c, S. Kulkarni^a, J. Downward^d, O. Perisic^e, R. L. Williams^e, L. Stephens^{a,2,3}, and P. T. Hawkins^{a,2,3}

^aThe Signaling Department, The Babraham Institute, CB22 3AT Cambridge, United Kingdom; ^bDepartment of Chemistry, University of Oxford, OX1 3QZ Oxford, United Kingdom; ^cThe Mass Spec Facility, The Babraham Institute, CB22 3AT Cambridge, United Kingdom; ^dThe Oncogene Biology Lab, The Francis Crick Institute, NW1 1AT London, United Kingdom; and ^eProtein and Nucleic Acid Chemistry, MRC Laboratory of Molecular Biology, CB2 0QH Cambridge, United Kingdom

Edited by Kevan M. Shokat, University of California, San Francisco, CA, and approved October 11, 2018 (received for review March 1, 2018)

Class IA PI3Ks have many roles in health and disease. The rules that govern intersubunit and receptor associations, however, remain unclear. We engineered mouse lines in which individual endogenous class IA PI3K subunits were C-terminally tagged with 17aa that could be biotinylated in vivo. Using these tools we quantified PI3K subunits in streptavidin or PDGFR pull-downs and cell lysates. This revealed that p85 α and β bound equivalently to p110 α or p110 β but p85 α bound preferentially to p110 δ . p85s were found in molar-excess over p110s in a number of contexts including MEFs (p85 β , 20%) and liver (p85 α , 30%). In serum-starved MEFs, p110-free-p85s were preferentially, compared with heterodimeric p85s, bound to PDGFRs, consistent with *in vitro* assays that demonstrated they bound PDGFR-based tyrosine-phosphorylated peptides with higher affinity and cooperativity; suggesting they may act to tune a PI3K activation threshold. p110 α -heterodimers were recruited 5–6 \times more efficiently than p110 β -heterodimers to activated PDGFRs in MEFs or PDGFR-based tyrosine-phosphorylated peptides in MEF-lysates. This suggests that PI3K α has a higher affinity for relevant tyrosine-phosphorylated motifs than PI3K β . Nevertheless, PI3K β contributes substantially to acute PDGF-stimulation of PIP₃ and PKB in MEFs because it is synergistically, and possibly sequentially, activated by receptor-recruitment and small GTPases (Rac/CDC42) via its RBD, whereas parallel activation of PI3K α is independent of its RBD. These results begin to provide molecular clarity to the rules of engagement between class IA PI3K subunits in vivo and past work describing “excess p85,” p85 α as a tumor suppressor, and differential receptor activation of PI3K α and PI3K β .

PI3K | Avi-tag | isoform-selective

Class IA PI3Ks are heterodimers with a regulatory (p85 α , p85 β , or p55 γ) and a catalytic subunit (p110 α , β , or δ , which give their name to a complex). They make the signaling lipid PIP₃ that is sensed by a range of effectors [e.g., protein kinase B (PKB), Bruton’s tyrosine kinase (BTK), PIP₃-dependent Rac exchange factor 1 (PRex1), PRex1] that control metabolism, the cytoskeleton, and growth. Genetic alterations that augment the activity of this network can advantage the survival of cancer cells and, consequently, the class I PI3K network is one of the most frequently mutated in cancer (1).

Work in the 1980s showed that the p85s and p110s bind “non-selectively” (2) and created the dogma that the relative abundance of the heterodimers is a function of their concentrations.

Class IA PI3Ks are activated by a variety of mechanisms, most characteristically by binding of the SH2 domains in p85s to “YXXM” phospho-tyrosines, in receptor tyrosine kinases (RTKs), their substrates, or adaptors (3). Dogma suggests that the properties of the SH2 domains in p85 α and β are sufficiently similar to drive parallel recruitment of p85s (despite exceptions, e.g., refs. 4 and 5).

A number of subunit and isoform specific interactions have been defined that underlie differences in the activation of the heterodimers; e.g., via the Ras Binding Domains (RBDs) in p110s [p110 α binds GTP-Ras- and p110 β binds GTP-Rac/CDC42-family

members (6, 7)] or the p110’s connections with the regulatory subunit’s SH2 domains [p110 β and p110 δ interact with both SH2 domains while p110 α only binds the N-SH2 (8)].

Analysis of wild-type and “oncomutant” class IA PI3Ks has revealed the principles governing their activation (8, 9). Interactions between the p85 subunits’ inter-SH2 domain with the p110s’ C2 domain, and the p85 subunits’ N-SH2 domain with the p110s’ helical, C2, and kinase domains inhibit kinase activity. In PI3K β and δ only, a contact between the C-SH2 and kinase domains also contributes (10). Phospho-tyrosine binding relieves inhibition by p85s. Class I PI3K activity is ultimately regulated by conformational transitions that increase membrane association and access to PI(4,5)P₂-substrate (11). Oncomutations mimic or facilitate the activation process in different ways (12, 13).

The class IA PI3K subunits are differentially expressed; p110 δ is abundant in immune cells, the remainder are ubiquitously but differentially expressed.

Work with PI3K inhibitors and GM-mice has cataloged p110-specific signaling in health and disease (1, 14). It is argued this arises

Significance

The class IA PI3Ks, comprised of regulatory (p85 α /p85 β /p55 γ) and catalytic (p110 α / β / δ) subunits, which make the signaling lipid PIP₃, constitute a key node in signaling. Many factors underlie their numerous cellular roles and large investments in the creation of PI3K-inhibitors. The existence of heterodimeric-isoforms (at least nine) with distinct distributions and properties and the often-debated existence of “p110-free-regulatory-subunits” as modulators provide the system with flexibility, redundancy and isoform-selective functions. Despite the scale of this endeavour, many of the system’s “rules of engagement” are unknown. Here we demonstrate preferential subunit associations, clarify the existence of “p110-free-regulatory-subunits”, show that they have properties that could allow them to modulate pathway activity, and reveal mechanisms that allow selective activation of PI3K α and β by receptors.

Author contributions: L.S. and P.T.H. designed research; N.T., T.N.D., T.C., S.M.S., and D.O. performed research; S.K., J.D., O.P., and R.L.W. contributed new reagents/analytic tools; N.T., T.N.D., T.C., S.M.S., D.O., L.S., and P.T.H. analyzed data; and N.T., T.N.D., T.C., S.M.S., R.L.W., L.S., and P.T.H. wrote the paper.

The authors declare no conflict of interest.

This article is a PNAS Direct Submission.

This open access article is distributed under [Creative Commons Attribution-NonCommercial-NoDerivatives License 4.0 \(CC BY-NC-ND\)](https://creativecommons.org/licenses/by-nc-nd/4.0/).

¹N.T., T.N.D., and T.C. contributed equally to this work.

²L.S. and P.T.H. contributed equally to this work.

³To whom correspondence may be addressed. Email: len.stephens@babraham.ac.uk or phillip.hawkins@babraham.ac.uk.

This article contains supporting information online at www.pnas.org/lookup/suppl/doi:10.1073/pnas.1803446115/-DCSupplemental.

Published online November 15, 2018.

because of differences in the properties and/or concentrations of p110s. However, this relies on the dogmas that there is little intersubunit selectivity and/or that p85s do not introduce specificity. The first of these assumptions has not been tested directly and the latter is contradicted by reports of differences in the properties of p85 α and p85 β (4, 5, 15, 16).

The concepts of p110-free and p110-independent functions of p85s have been raised many times, including a recent report that *PIK3R1* (encoding p85 α) can be a tumor suppressor (17–22) and evidence that p110-free p85s are targeted for isoform-specific degradation (18, 23). Some work has provided evidence for specific p110-free regulatory subunit complexes (19); however, the best quantitative analysis of class IA PI3K subunit stoichiometry concluded there were no p110-free regulatory subunits (24). We have addressed these questions/debates.

Results

We used standard homologous targeting technology in mouse ES cells to derive mouse strains expressing either the biotin ligase mBirA [the prokaryotic biotin ligase BirA modified to have mammalian codon usage (25)] from the endogenous ROSA26 locus (mBirA^{+/+}) or endogenous, C-terminal avi-tagged [17aa, containing a 15aa minimal consensus for BirA (26)] p85 α , p85 β , p110 α , p110 β , or p110 δ (e.g., p85 α ^{avi/avi}, which will tag all three splice-variants of p85 α), all in a C57BL/6J background (*SI Appendix, Figs. S1–S7*). The mice were interbred to express mBirA or the avi-tagged alleles alone or together (e.g., mBirA^{+/+}, p85 α ^{avi/avi} x mBirA^{+/+}). All of these strains appeared healthy and fertile except p110 α ^{avi/avi}-mice that did not reach adulthood. The majority died just before birth [p110 α ^{KD/KD} mice die near E10 (27)]. It seems likely, on the basis of the results below, that this problem is due to the C-terminal avi-tag reducing, but not abating, the kinase activity of p110 α ; a phenomenon that has been

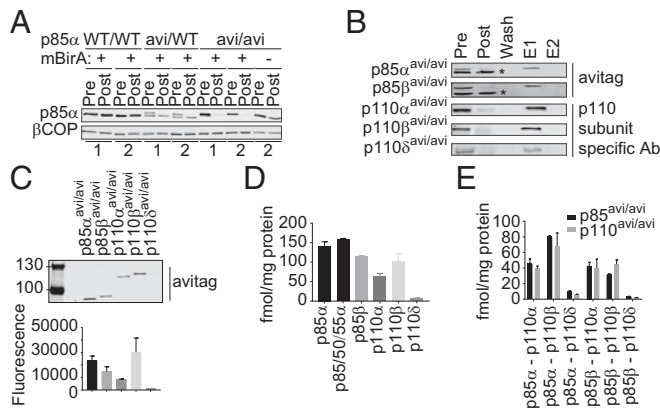


Fig. 1. Absolute quantitation of class IA PI3K subunits and heterodimers in MEFs. (A) Immunoblot of endogenous p85 α in lysates of MEFs (clones 1 or 2, genotypes indicated) before (pre) or after (post) pull-down with streptavidin beads. β COP is a loading control. (B) Immunoblots (antibodies noted right) of MEF lysates (genotypes indicated left, all expressing mBirA) before or after pull-down with streptavidin beads compared with aliquots of the bead-wash, the 1st eluate (E1, SDS sample buffer) and 2nd eluate (E2). Nonspecific bands are marked *. (C) An anti-avi-immunoblot (fluorescent 2nd Ab) of MEF lysates (genotypes indicated). Histogram shows quantification (means \pm SD, from two independent MEF clones/genotype) corrected for input protein. (D) Absolute quantitation of avi-tagged-PI3K subunits by streptavidin pull-down and mass spec and corrected for input protein (means, \pm SD, from two independent clones/genotype, each clone was measured three times, see *SI Appendix, Fig. S11*). (E) Absolute levels of the class IA PI3K heterodimers, measured by streptavidin pull-down, from MEF lines expressing avi-tagged p85 (grey bars) or p110 (black) proteins, and mass spec and corrected for input protein (means, \pm SD, from two independent MEF clones/genotype, each clone was measured three times). Independent estimates of the amount of each heterodimer are derived from the p85- or p110-directed pull-downs. The underlying data are in *SI Appendix, Fig. S11*.

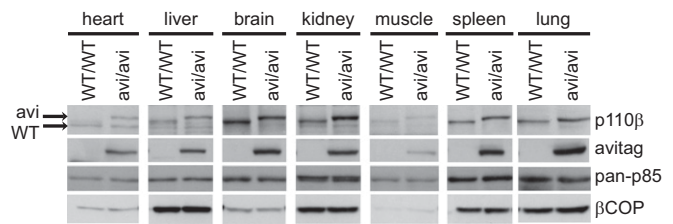


Fig. 2. Avi-tagging leads to a band-shift but unchanged expression of endogenous p110 β in various mouse tissues. Lysates from indicated mouse tissues from p110 β ^{WT/WT} or p110 β ^{avi/avi} mice were resolved by SDS/PAGE and immunoblotted with the indicated antibodies.

reported before for other C-terminal tags (28). We derived MEFs from mice expressing each of the avi-tagged subunits and introduced mBirA (or not) and EGFP via viral transduction and sorted EGFP-positive cells for experiments (Fig. 1A).

Tissue or cell lysates were prepared and subjected to streptavidin-directed pull-down under mild, nondenaturing conditions. Aliquots of the lysates before and after pull-down were immunoblotted with antibodies recognizing: the avi-tag, p85 α , p110 α , p110 β , or p110 δ (Figs. 1A–D and Fig. 2; see also *SI Appendix, Figs. S3–S7*). The avi-tagged and/or biotinylated constructs resolved from the endogenous proteins. Firstly, this made it clear, by internal comparison of wild-type and avi-tagged proteins in avi-heterozygous cells/tissues (e.g., p85 α -immunoblots of p85 α -avi-expressing MEFs, Fig. 1A) or in avi-homozygous cells/tissues (e.g., p110 β -immunoblots of p110 β -avi-expressing mouse tissues, Fig. 2) that the presence of the avi-tag had no effect on expression of any of the class IA PI3K subunits (for p85 β and p110 δ blots, see *SI Appendix, Figs. S4 and S7*). Secondly, this made it possible to detect complete streptavidin-directed pull-down of avi-tagged, but not wild-type, proteins in the presence, but not the absence, of mBirA (Fig. 1A and B). These latter results demonstrate near 100% mBirA- and avi-tag-dependent biotinylation and then streptavidin-mediated pull-down.

As the expression of the PI3K subunits was unchanged by avi-tagging, it seemed unlikely their turnover had been perturbed. This was confirmed in “chase” experiments in the presence of an inhibitor of protein synthesis (emetine) with p85 α ^{avi/WT}-MEFs that revealed the rate of degradation of endogenous avi-tagged p85 α was indistinguishable from wild-type-p85 α in the same cells (*SI Appendix, Fig. S8A*). Furthermore, MEFs expressing avi-tagged p85 α (p85 α ^{avi/avi}) produced near-identical amounts of PIP₃, in response to either PDGF or EGF, as wild-type control-MEFs (*SI Appendix, Fig. S8B*). Together these results show that avi-tagging the class IA PI3K subunits did not perturb their levels or turnover and had limited effects on function.

Quantification of anti-avi immunoblots revealed that p85 α and p110 β are the major isoforms of the regulatory and catalytic subunits in MEFs (Fig. 1C), confirming earlier work (24). We also quantified the expression of the individual avi-tagged subunits in cell lines expressing the relevant avi-tagged proteins by streptavidin pull-down, elution, and mass spectrometry in the presence of multiple, internal, heavy-labeled, synthetic peptide standards to correct for recovery (Fig. 1D and *SI Appendix, Figs. S9–S11*). This confirmed the results with anti-avi immunoblots and indicated the levels of p85 α (almost exclusively the largest variant) and p110 β to be 58,000 or 42,000 molecules/cell, respectively (intracellular concentrations of 32 or 23 nM). Deeper analysis of these pull-downs (using the heavy-peptide standards) allowed us to quantify all of the other class IA PI3K subunits that were recovered in the pull-downs and hence obtain two (from the p85^{avi/avi} or p110^{avi/avi}-pull-downs) independent, direct estimates for the absolute concentration of each heterodimer (Fig. 1E and *SI Appendix, Fig. S11A*). The relative concentrations of heterodimers were: p85 α /p110 β > p85 α /p110 α = p85 β /p110 α = p85 β /p110 β >> p85 α /p110 δ & p85 β /p110 δ . Very low levels of p55 γ were recovered with avi-tagged p110 α or β , in keeping with

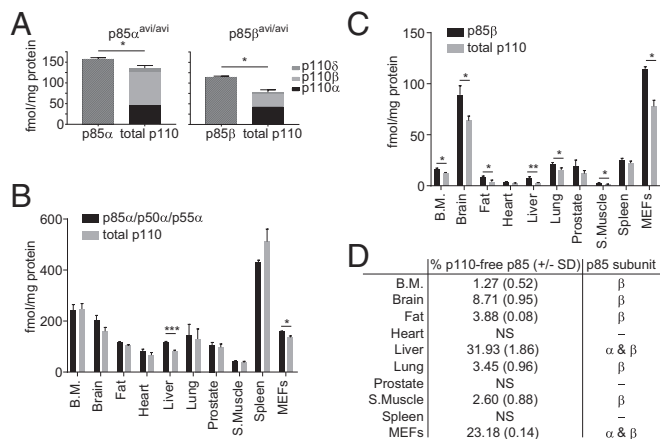


Fig. 3. p110-free p85 is present in MEFs and certain murine tissues. (A) The absolute amounts of avi-tagged p85s compared with the amount of p110s recovered with them in streptavidin pull-downs from p85 α ^{avi/avi} or p85 β ^{avi/avi} MEFs, corrected for input protein (means, \pm SD, from two clones/genotype, each clone was measured three times). (B and C) Experiments like those in A except using tissues from mice expressing avi-tagged p85s and mBirA. Data are corrected for input protein (means \pm SD, from three independent mice). (D) The percentage of total p110-free p85 in different mouse tissues was calculated from results shown in A–C. Statistically significant at * P < 0.05, ** P < 0.01, and *** P < 0.001. NS, not significant. The underlying data are in *SI Appendix, Fig. S11*.

its tissue distribution. The results also indicate that the avi-tags had minimal impact on intersubunit associations.

These experiments also enabled us to measure p110-free p85s and the selectivity of intersubunit associations in vivo. By measuring the total moles of the different p110s in p85 α ^{avi/avi} or p85 β ^{avi/avi}-pull-downs from MEFs (Fig. 3A and *SI Appendix, Fig. S11A*) and various mouse tissues (Fig. 3B and C and *SI Appendix, Fig. S11B*), we could calculate the percentage of p110-free p85 in these contexts (Fig. 3D). This revealed that in liver and MEFs there is significant p110-free p85 α and/or p85 β .

We also measured the stoichiometry of p85 α and p85 β found in individual p110-avi-pull-downs compared with their total concentrations in MEFs, and that of p110s found in individual p85-avi-pull-downs in mouse spleen or bone marrow (where p110 δ is highly expressed) (Fig. 4A and B and *SI Appendix, Figs. S11 and S12*). These results indicated that p110 α and p110 β associate with p85 α and p85 β nonselectively. However, more p110 δ is recovered with p85 α than its concentration predicts and hence appears to bind p85 α selectively. We independently confirmed these results by immunoblotting for p110 δ and p85 α in lysates from spleens (from p85 α ^{avi/avi} or p85 β ^{avi/avi} mice) before and after streptavidin-mediated pull-down (Fig. 4C).

PDGFRs are composed of PDGFR α and PDGFR β subunit dimers and bind to class IA PI3K regulatory subunits through a pair of autophosphorylated tyrosine residues in the cytoplasmic kinase-insert domain. We measured ligand-dependent association of class IA PI3K subunits with PDGFRs in MEFs by immunoprecipitation (IP) of the receptors (with about 80–90% efficiency Fig. 5A) and immunoblotting or mass spectrometry with internal, heavy-peptide standards (Fig. 5B–D). Very similar proportions of total p85 α and p85 β became associated with PDGFRs in PDGF-stimulated MEFs (Fig. 5B–D), whether measured by immunoblotting or mass spectrometry (when the latter data were corrected for the absolute amounts of p85 α and p85 β in the MEFs, see *SI Appendix, Fig. S12*). This was true across a range of doses of PDGF (Fig. 5C and D) and suggests that PDGFRs have quantitatively similar interactions with p85 α or p85 β . Interestingly, following submaximal stimulation, p110 α was recruited to activated PDGFRs five to six times more effectively than p110 β (i.e., correcting for the cellular concentrations of the p110s, Fig. 5B–D and *SI Appendix, Fig. S12*). This result indicated that p110 α , compared with p110 β , containing

class IA PI3K complexes are selectively recruited to activated PDGFRs. This selectivity appeared to be largely intrinsic to the PI3K-complexes, and not a result of, e.g., compartmentalization or associations that are not via SH2 domain:phospho-tyrosine interactions, as the proportions of endogenous PI3K α and PI3K β in MEFs lysates were similarly, and almost completely, bound by excess concentrations of doubly tyrosine phosphorylated peptides based on activated murine PDGFRs (PYP, 5,000 fmol, Fig. 5E and F).

These results suggest the catalytic subunits of class IA PI3Ks have a powerful impact on recruitment to tyrosine-phosphorylated proteins. The C-SH2 domain of p85 subunits bind (involving Y685 in p85 α) and restrain the activity of p110 β and δ , but not p110 α , heterodimers in the absence of phospho-tyrosine docking (8). This might lead to the C-SH2 in PI3K α having higher affinity for activated PDGFRs and hence could explain our results. To test this, we did experiments with recombinant PI3K α and β in which recovery of wild-type-p85 α -containing or Y685A-p85 α -containing PI3K α or PI3K β with biotinylated PYPs in streptavidin-pull-downs was measured. We found that Y685A-p85 α -increased, compared with wild-type p85 α , the recovery of p110 β , but not p110 α -containing heterodimers (*SI Appendix, Fig. S13A*), consistent with work measuring activation of similar constructs by PYPs (8, 10). However, we saw little difference between the recovery of the recombinant PI3K α and PI3K β . This result was supported by equilibrium binding experiments that indicated recombinant PI3K α and PI3K β have similar affinities for PYPs (*SI Appendix, Fig. S13B*). These results suggest that the apparently greater freedom of the C-SH2 domain in PI3K α is not the prime reason for the higher recovery of endogenous PI3K α than PI3K β with activated PDGFRs. We cannot explain the difference in the behavior of the endogenous and recombinant PI3K α and β complexes in these assays. There may be posttranslational modifications to PI3K α / β in MEFs that lead to PI3K α having a relatively higher affinity for activated PDGFRs.

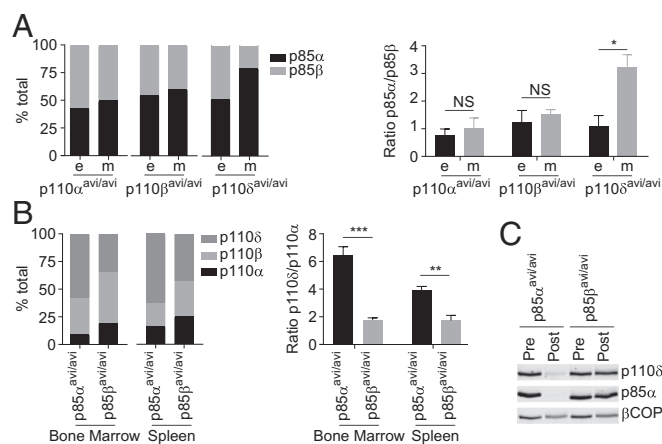


Fig. 4. p85 α and p110 δ , but not other subunits, interact preferentially in vivo. (A) Compares the expected (e) and the measured (m), by streptavidin pull-down and mass spec, levels of the different class IA PI3K heterodimers in MEFs. Expected levels were calculated based on total p85 levels in the respective MEFs (*SI Appendix, Fig. S12*) accounting for the percentage of p85 α or β not bound to p110 (Fig. 3); expressed as percentages of the total p85. Data are means \pm SD, from two MEF clones/genotype. (B) The levels of p110 subunits bound to p85 α or β in the bone marrow or spleen of mice expressing relevant avi-tagged PI3K constructs. The levels are expressed as percentages of the total p110 measured by mass spec. Data shown are means \pm SD, from three mice. (C) The levels of p110 δ in lysates of spleens from mice expressing mBirA and either avi-tagged p85 α or β , before (pre) and after (post) streptavidin pull-down, as assessed by immunoblotting. Parallel immunoblots for p85 α and β COP, that control for the efficiency of pull-down and cell-input, are also shown. The data are from a typical experiment repeated twice. Statistically significant at * P < 0.05, ** P < 0.01, and *** P < 0.001. NS, not significant.

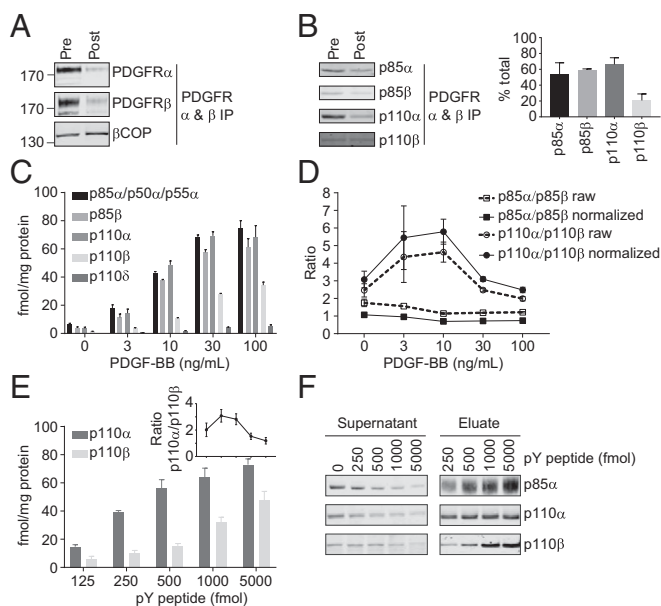


Fig. 5. p110 α is preferentially recruited to activated PDGFRs. (A) The levels of PDGFR α and β in MEF lysates (clone WT #1) before (pre) and after (post) pull-down with anti-PDGFR Abs was measured by immunoblotting, with β COP as a loading control. (B) Relative levels of PI3K subunits recruited to PDGFRs following stimulation with PDGF-BB (10 ng/mL for 1 min). Representative immunoblots before and after PDGFR pull-down (Left) and quantitation of each subunit's recruitment, as a percentage of its total level in that clone (clone WT #1, *SI Appendix*, Fig. S12). (C) The absolute levels of subunits recruited to PDGFRs following stimulation with different doses of PDGF-BB for 1 min, measured by mass spec. (D) "Raw" ratios of p110 α /p110 β and p85 α /p85 β associated with PDGFRs, based on measurements in C. Normalized ratios were calculated by dividing the raw ratios by the ratios of the total levels of those subunits in that clone of MEFs as calculated in *SI Appendix*, Fig. S12. (E) Absolute levels of p110 α and p110 β recovered with a PYP; the *Inset* shows the normalized (based on *SI Appendix*, Fig. S12) ratio of p110 α /p110 β recovered with tyrosine-phosphorylated peptides. (F) Immunoblots of PI3K subunits in lysates following pull-down with the PYPs or eluted from those pull-downs. The data are all means, \pm SD, from three independent experiments.

Quantitative analyses of class IA PI3K subunits in PDGFR-IPs from MEFs also found evidence for p110-free p85 (Fig. 6 A–C and *SI Appendix*, Fig. S14). Because of the context of these assays, we could only measure the total, PDGFR-associated p110-free p85 but not the proportions that were p85 α or p85 β . Significantly, PDGFRs were enriched in p110-free p85, compared with heterodimeric p85, under basal unstimulated conditions and in the presence of low concentrations of PDGF (Fig. 6 A and B). Consistent with this, the proportion of p110-free p85 β ^{avi/avi} that could be recovered by streptavidin from lysates of p85 β ^{avi/avi}-expressing MEFs was reduced by prior IP of PDGFRs (Fig. 6C). These results suggest that p110-free p85 has a higher affinity than heterodimeric-p85 for tyrosine-phosphorylated PDGFRs. This hypothesis was confirmed by *in vitro* binding experiments (Fig. 6D) which showed that p85 α bound PYPs with higher affinity and co-operativity than p85 α /p110 α .

PDGF stimulates a transient accumulation of PIP₃ leading to phosphorylation of PKB in MEFs (7, 29). Activation of PKB has been shown to be substantially reduced, at lower doses of PDGF, in p110 α ^{-/-}, but not p110 β ^{-/-}, MEFs (29, 30). Given our results suggesting PI3K α and β are both, although differentially, recruited to PDGFRs, we determined their roles in PDGF-stimulated PIP₃ accumulation in MEFs. BYL-719 inhibited PIP₃ accumulation (Fig. 7A) by about 60% at concentrations that are likely to be PI3K α -selective (<1 μ M). TGX-221, at concentrations consistent with its action being on PI3K β (<0.1 μ M),

inhibited PIP₃ accumulation (Fig. 7A and B) by about 40%. This inhibition was manifest across a range of PDGF concentrations (Fig. 7B) and further increased by a submaximal inhibitory dose of PI3K α -selective inhibitor (Fig. 7A). Interestingly, although TGX-221 inhibited PDGF-stimulated PKB phosphorylation, it did so only at lower concentrations of PDGF (Fig. 7C), consistent with previous data (30) and the idea that PKB phosphorylation can be maximally activated by submaximal amounts of PIP₃. These results suggest that PI3K α and PI3K β are both activated by PDGFRs and that they have both unique and overlapping roles in PIP₃ accumulation.

The quantitatively similar roles of PI3K α and PI3K β in PIP₃ accumulation contrasted with the preferential recruitment of PI3K α to PDGFRs. To understand if this was a result of a difference in their regulation by small GTPases, we obtained MEFs from mice expressing small-GTPase-insensitive, point-mutant knock-ins of p110 α and p110 β [Ras-insensitive-p110 α , p110 α ^{T208D, K227A/T208D, K227A} (7) and Rac/CDC42-insensitive-p110 β , p110 β ^{S205D, K224A/S205D, K224A} (6)]. Mice, and MEFs derived from them, expressing these constructs have been used to reveal important roles for the RBDs of PI3Ks α & β in tumorigenesis and some G protein-coupled receptor (GPCR) signaling via class I PI3Ks (6, 7). We measured PDGF-stimulated PIP₃ accumulation in these MEF lines and the association, of both the wild-type and small-GTPase-insensitive versions, of p110 α and p110 β with PDGFRs. We found that the RBD of p110 α was not needed for PDGF-stimulated PIP₃ accumulation (Fig. 8A), consistent with previous work measuring PKB phosphorylation (7). In contrast, the RBD of p110 β was required for maximal PDGF-stimulated PIP₃ accumulation [Fig. 8B and C; work indicating the RBD of p110 β is not required for PDGF-stimulated AKT phosphorylation (6) used 5 min stimulations and is entirely consistent with our results showing the role of the RBD is reduced at later times, Fig. 8B)]. A comparison of the effect of a PI3K β -selective

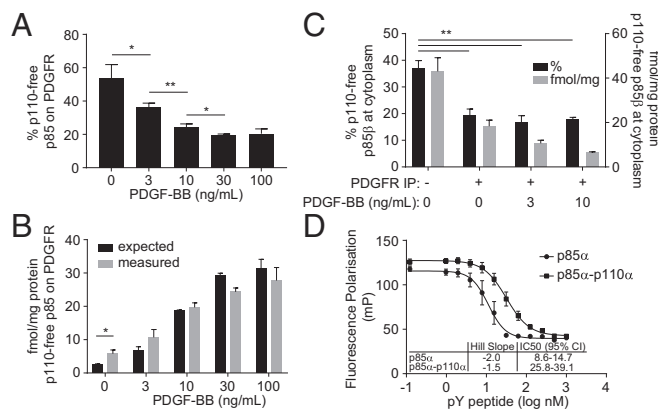


Fig. 6. p110-free p85 is recruited to PDGFRs with higher affinity than the p85-p110 dimers at low levels of receptor activation. (A) The amounts of p110-free p85 associated with PDGFRs following stimulation with PDGF-BB (1 min). Levels are expressed as a percentage of the total p85 associated with PDGFRs (as presented in Fig. 5). (B) Absolute amounts of p110-free p85 recovered with PDGFRs, quantified by mass spec ("measured") compared with the amount predicted if no difference in affinity, between p110-free and heterodimeric-p85, existed ("expected"). Expected values were calculated by multiplying the amount of total p85 recruited to PDGFR (Fig. 5C) with the percentage p110-unbound p85 in that clone (Fig. 3D). (C) Amounts of p110-free p85 β in streptavidin pull-downs from MEFs expressing p85 β ^{avi/avi}, with (+) or without (–) prior pull-down of PDGFRs. The amount is expressed as a percentage of the total amount of p85 β pulled down or as absolute levels. (D) Estimating the apparent affinity of interaction between recombinant, purified, monomeric p85 α or p85 α -p110 α dimers and PYPs using fluorescence polarization. A given protein preparation was equilibrated with a fluorescein-labeled PYP (Fluor-GpYMDMS, 2 nM) and a doubly phosphorylated, nonfluorescent PYP was titrated into the mixture to the indicated concentrations. The data are all means, \pm SD, from three independent experiments. Statistically significant at * P < 0.05 and ** P < 0.01.

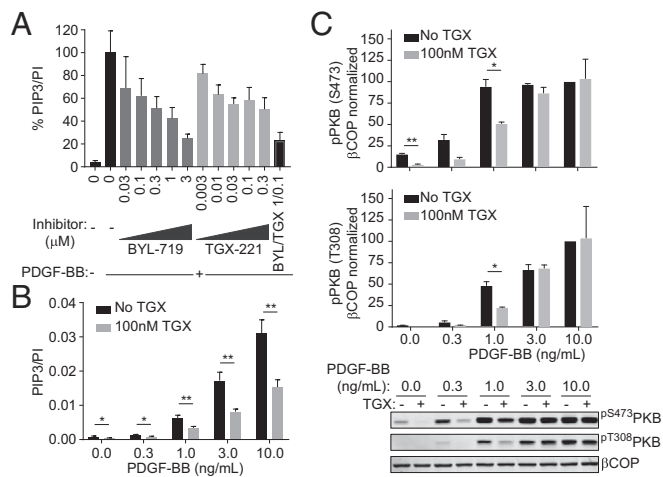


Fig. 7. Despite a relatively small amount of PI3K β being associated with activated PDGFRs, it generates a more substantial proportion of the PIP₃ that accumulates. (A) Inhibition of PDGF-stimulated (PDGF-BB, 10 ng/mL, 1 min) PIP₃ accumulation by p110 α -selective (BYL-719) and/or p110 β -selective (TGX-221) inhibitors in MEFs. The data are means, \pm SD, from three experiments. (B) Impact of TGX-221 on PIP₃ levels following stimulation with various doses of PDGF-BB for 1 min. The data are means, \pm SD, from three experiments. (C) Impact of TGX-221 on phosphorylation of PKB following stimulation with various doses of PDGF-BB for 1 min assessed by immunoblotting with anti-phospho- T308 or S473-antibodies. Results were corrected for cell input using β COP and expressed as percentages of P-PKB following 10 ng/mL PDGF-BB. The data are means, \pm SEM, from two experiments. * P < 0.05, ** P < 0.01 (t test, two-sample equal variance, two-sided distribution).

inhibitor on PDGF-stimulated PIP₃ accumulation in MEFs expressing either wild-type- or Rac/CDC42-insensitive versions of p110 β , suggested that p110 β is substantially dependent on its RBD in this context (Fig. 8C).

To understand the role of the RBD in p110 α and p110 β association with, and activation by, PDGFRs we measured the recovery of these constructs with PDGFRs by mass spectrometry. We found that the ligand-stimulated association of p110 α with PDGFRs was not dependent on its RBD's ability to bind to Ras (Fig. 8D and *SI Appendix*, Fig. S15). These results confirm previous work indicating neither growth factor-stimulated PKB phosphorylation nor association of p85s with tyrosine-phosphorylated proteins are dependent on Ras binding to the RBD of p110 α (7). Surprisingly, however, the results also showed that despite the very clear role for the RBD of p110 β in PDGF-stimulated PIP₃ accumulation, it had no role in binding of PI3K β to PDGFRs. The simplest explanation for these results is that Ras does not contribute to activation of PI3K α at PDGFRs, whereas binding of active Rac/CDC42 is absolutely required for stimulation, but not binding, of PI3K β at PDGFRs.

Discussion

Our results show that p85 α and p85 β bind p110 α or p110 β with indistinguishable affinity *in vivo* and hence the concentrations of the heterodimers they can form are solely a function of the relative levels of the subunits. Interestingly, p110 δ preferentially complexes with p85 α compared with p85 β . These results suggest that PI3K δ is hard-wired to use p85 α - or avoid p85 β -specific properties or functions; e.g., phosphorylation (15) or p85 β -directed (18) or 85 α -directed (23) ubiquitination and degradation. It is noteworthy that the phenotypes of mice lacking p85 α or expressing kinase-dead p110 δ are most similar in B lymphocytes where PI3K δ is dominant (31, 32). Hence our data resolve an important long-standing question about the rules of engagement in class IA PI3K signaling (9).

We find that p85 α and p85 β contribute very similar PDGFR-binding capabilities to class IA PI3Ks. This is consistent with the known similarities in phospho-peptide-binding properties of the N and C-terminal SH2 domains within and between class IA PI3K

regulatory proteins (3). Reported differences in the properties of p85 α and p85 β , in different contexts (4, 5), are presumably due to other interactions and/or domains.

Our data, derived from analysis of both p85- and PDGFR-pull-downs, suggest that p110-free p85 α and p85 β are present in mouse tissues and cells. This provides direct, independent support for recent work identifying roles for p110-free p85s (19, 21, 22). p110-free p85s have higher affinity and more co-operative binding to tyrosine-phosphorylated proteins than heterodimeric p85 proteins. This property could allow relatively small amounts of p110-free p85s to compete effectively with heterodimeric PI3Ks for low-abundance phosphorylated YXXM motifs. This may explain their relative enrichment on PDGFRs in basal or weakly stimulated cells and suggests they may have a role in reducing basal RTK signaling noise and/or in setting a threshold level of receptor activation that must be achieved to drive class IA PI3K activation. The stoichiometry of p85s to potential phospho-tyrosine binding sites will be an important determinant of the impact of p110-free p85s on PI3K signaling. A large excess of tyrosine-phosphorylated "YXXM" proteins over p85s would suggest that the window in which p110-free p85 might act as an inhibitor would be very limited. The stoichiometry with which tyrosine residues in endogenous proteins are phosphorylated is difficult to measure. However, given that a number of YXXM-containing signaling proteins seem to have similar copies per cell as p85s [PDGFRs, EGFRs, insulin receptor substrates (IRs) in MEFs are all in the range 1×10^4 – 2×10^5 compared with 10^5 p85s] and maximal PDGFR activation leads to over 80% of total p85 associating with anti-PDGFR-IPs (Fig. 5B and C), it seems that upon intense challenge there will be an excess of phosphorylated YXXM motifs and depletion of cytosolic p85s. Hence, p110-free

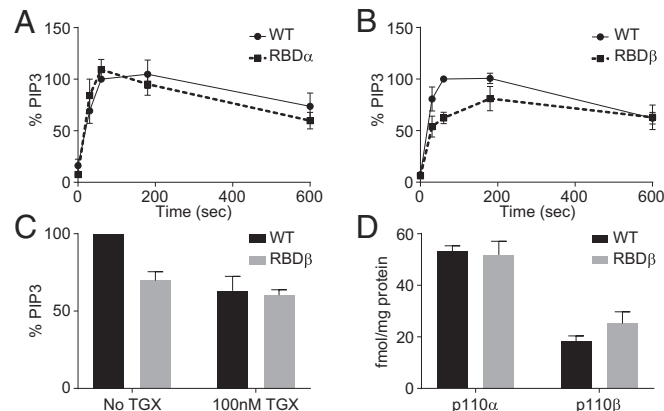


Fig. 8. The RBD domain of p110 β is necessary for PIP₃ production but not for binding to activated PDGFRs. (A) PDGF-stimulated (PDGF-BB, 10 ng/mL, 1 min) PIP₃ accumulation in MEFs expressing wild-type (WT) or Ras-insensitive p110 α (RBD α). Results are expressed as percentage of the PIP₃ levels in the respective, wild-type (WT) line. The data are means, \pm SEM, from three experiments. (B) PIP₃ accumulation in MEFs expressing WT or Rac/CDC42-insensitive p110 β (RBD β). Data are expressed as in A. The amount of PIP₃ that accumulated in MEFs expressing RBD β , but not RBD α , was significantly lower than their WT controls (P = 0.011, two-way ANOVA). (C) PIP₃ levels in PDGF-stimulated (PDGF-BB, 10 ng/mL, 1 min) WT or RBD β -MEFs in the presence, or absence, of TGX-221 (100 nM). Results are expressed as percentage of the PIP₃ levels measured in the respective WT-MEFs in the absence of inhibitor. The data presented are means, \pm SD, from three experiments, TGX-221 significantly inhibited the response in WT- (P = 0.03, ratio paired t test) and RBD β -MEFs (P = 0.03, ratio paired t test). (D) The absolute amounts of p110 α or p110 β recruited to activated PDGFRs (PDGF-BB, 10 ng/mL for 1 min) in RBD β - or WT-MEFs. The data are presented as means, \pm SD, from three experiments, the amount of p110 β associated with the activated PDGFRs was significantly lower than p110 α (P = 0.00003 in WT and 0.0027 in RBD β -MEFs; t test, two-sample equal variance, two-sided distribution); however, the association of neither p110 α nor p110 β was significantly changed in the context of the RBD β mutant construct. The data underlying D is shown in *SI Appendix*, Fig. S15.

p85 could act to tune the threshold, but not the maximal, activation of class IA PI3K signaling.

Although PI3K α played the major role in PDGF-stimulated PIP₃ synthesis, PI3K β generated a disproportionately larger amount than predicted by its association with PDGFRs. We speculated this might be a result of a difference in other signals integrated by PI3K α and PI3K β . Our data show that binding of active Ras to the RBD of p110 α is not needed for PDGF-stimulated association of PI3K α with PDGFRs or for PIP₃ accumulation. In contrast, the equivalent binding of Rac/CDC42 to the RBD of p110 β is required for PDGF-stimulated PI3K β -dependent PIP₃ accumulation but not for association of PI3K β with PDGFRs. The simplest explanation of the latter results is that, in vivo, PI3K β is extremely dependent on combined activation by Rac/CDC42 and the activated PDGFR, in line with a previous hypothesis (33). The two inputs to PI3K β could be engaged in any order. The most parsimonious explanation of our data is that they act sequentially, because of a requirement for PI3K β to be associated with PDGFRs to become sensitive/accessible to Rac/CDC42 (34). In this model, the role of Rac/CDC42 might be to allow PDGFR-associated PI3K β access to PI(4,5)P₂.

Our results resolve some long-standing questions and also raise further questions regarding the origin of the selective interaction between p85 α and p110 δ and the physiological purpose of p110-free p85 α and p85 β . It will also be important to extend our studies describing preferential recruitment of PI3K α versus PI3K β to tandem phospho-tyrosines in PDGFRs to other contexts involving different local sequences and numbers of phospho-tyrosine binding sites.

Materials and Methods

Generation of PI3K-Avi-Tag and mBirA Mice. *Pik3ca-avi*, *Pik3cb-avi*, *Pik3cd-avi*, *Pik3r1-avi*, *Pik3r2-avi*, and *Rosa26-mBirA* targeting vectors were generated by a combination of cloning, recombineering, and gene synthesis and used to generate mice expressing avi-tagged PI3K subunits homozygotes (except live p110 α ^{avi/avi}) and *Rosa26-mBirA* heterozygotes on a pure C57BL/6J background by standard ES cell manipulation and breeding (SI Appendix, Materials and Methods and Figs. S1–S7). The Babraham Institute's Animal Welfare and

Ethical Review Body, which includes veterinary experts and members of the public, approved the animal experiments described in the manuscript.

MEF Preparation, Cell Culture, and Lysis. Primary MEFs were derived from 14.5 d old embryos and immortalized with SV40T (SI Appendix).

Growth Factor Stimulations. MEFs were serum-starved 16 h then stimulated with recombinant murine PDGF-BB with doses and for times indicated in the figures. PI3Ks inhibitors were added 20 min before stimulation.

Quantification of PI(3,4,5)P₃. Lipid extraction and absolute quantitation of PI(3,4,5)P₃ levels in 2 × 10⁵ cell aliquots of MEFs were analyzed by published methods (35).

Pull-Down of Class IA PI3K with PYPs. PI3Ks were recovered from MEF lysates using a synthetic, biotinylated, doubly phosphorylated peptide derived from murine PDGFR (PYP, residues 735–767) and streptavidin-mediated pull-down.

Association of Recombinant PI3K Complexes with PYPs. Recombinant PI3K heterodimers (p85 α /p110 α , p85 α /p110 β , p85 α -Y685A/p110 α , and p85 α -Y685A/p110 β) were expressed in Sf9 cells, purified, and various amounts were incubated with biotin-labeled doubly phosphorylated PYP, pulled down with streptavidin beads, and the associated p85 α was quantified by immunoblotting with fluorescent 2^o antibodies as described in the SI Appendix.

Matters only Described in the SI Appendix. Antibodies and Reagents. Immunoblotting. Streptavidin- and antibody-mediated pull-down. Sample preparation and analysis by mass spectrometry and absolute protein quantitation. Preparation of recombinant PI3Ks. Competition Assays with PYPs. Statistics.

ACKNOWLEDGMENTS. This work was supported by grants from the Biotechnology and Biological Sciences Research Council (BBSRC) [BB/J004456/1 (to L.S. and P.T.H.)] all Babraham Institute facilities are supported by a Core Capability Grant, Wellcome Trust [WT085889MA (to L.S. and P.T.H.)] and Medical Research Council [MR/R000409/1 (to T.C., L.S., and P.T.H.)] and MC_U105184308 (to R.L.W.). We thank Dr. U. Mechold and Prof. V. Ogryzko for mBirA cDNA and Dr. W. Dean for ZP3-Cre mice.

- Thorpe LM, Yuzugullu H, Zhao JJ (2015) PI3K in cancer: Divergent roles of isoforms, modes of activation and therapeutic targeting. *Nat Rev Cancer* 15:7–24.
- Vanhaesebroeck B, et al. (1997) P110delta, a novel phosphoinositide 3-kinase in leukocytes. *Proc Natl Acad Sci USA* 94:4330–4335.
- Sonyang Z, et al. (1993) SH2 domains recognize specific phosphopeptide sequences. *Cell* 72:767–778.
- Hartley D, Meisner H, Corvera S (1995) Specific association of the beta isoform of the p85 subunit of phosphatidylinositol-3 kinase with the proto-oncogene c-cbl. *J Biol Chem* 270:18260–18263.
- Alcázar I, et al. (2009) p85beta phosphoinositide 3-kinase regulates CD28 coreceptor function. *Blood* 113:3198–3208.
- Fritsch R, et al. (2013) RAS and RHO families of GTPases directly regulate distinct phosphoinositide 3-kinase isoforms. *Cell* 153:1050–1063.
- Gupta S, et al. (2007) Binding of ras to phosphoinositide 3-kinase p110alpha is required for ras-driven tumorigenesis in mice. *Cell* 129:957–968.
- Burke JE, Williams RL (2013) Dynamic steps in receptor tyrosine kinase mediated activation of class IA phosphoinositide 3-kinases (PI3K) captured by H/D exchange (HDX-MS). *Adv Biol Regul* 53:97–110.
- Backer JM (2010) The regulation of class IA PI 3-kinases by inter-subunit interactions. *Curr Top Microbiol Immunol* 346:87–114.
- Zhang X, et al. (2011) Structure of lipid kinase p110 β /p85 β elucidates an unusual SH2 domain-mediated inhibitory mechanism. *Mol Cell* 41:567–578.
- Hon WC, Berndt A, Williams RL (2012) Regulation of lipid binding underlies the activation mechanism of class IA PI3-kinases. *Oncogene* 31:3655–3666.
- Miled N, et al. (2007) Mechanism of two classes of cancer mutations in the phosphoinositide 3-kinase catalytic subunit. *Science* 317:239–242.
- Burke JE, Perisic O, Masson GR, Vadas O, Williams RL (2012) Oncogenic mutations mimic and enhance dynamic events in the natural activation of phosphoinositide 3-kinase p110 α (PIK3CA). *Proc Natl Acad Sci USA* 109:15259–15264.
- Vanhaesebroeck B, Guillermet-Guibert J, Graupera M, Bilanges B (2010) The emerging mechanisms of isoform-specific PI3K signalling. *Nat Rev Mol Cell Biol* 11:329–341.
- Reif K, Gout I, Waterfield MD, Cantrell DA (1993) Divergent regulation of phosphatidylinositol 3-kinase P85 alpha and P85 beta isoforms upon T cell activation. *J Biol Chem* 268:10780–10788.
- Oak JS, Chen J, Peralta RQ, Deane JA, Fruman DA (2009) The p85beta regulatory subunit of phosphoinositide 3-kinase has unique and redundant functions in B cells. *Autoimmunity* 42:447–458.
- Ueki K, Algenstaedt P, Mauvais-Jarvis F, Kahn CR (2000) Positive and negative regulation of phosphoinositide 3-kinase-dependent signaling pathways by three different gene products of the p85alpha regulatory subunit. *Mol Cell Biol* 20:8035–8046.
- Kuchay S, et al. (2013) FBXL2- and PTPL1-mediated degradation of p110-free p85 β regulatory subunit controls the PI(3)K signalling cascade. *Nat Cell Biol* 15:472–480.
- Winnay JN, Boucher J, Mori MA, Ueki K, Kahn CR (2010) A regulatory subunit of phosphoinositide 3-kinase increases the nuclear accumulation of X-box-binding protein-1 to modulate the unfolded protein response. *Nat Med* 16:438–445.
- Chagpar RB, et al. (2010) Direct positive regulation of PTEN by the p85 subunit of phosphatidylinositol 3-kinase. *Proc Natl Acad Sci USA* 107:5471–5476.
- Cheung LW, et al. (2015) Regulation of the PI3K pathway through a p85 α monomer-homodimer equilibrium. *eLife* 4:e06866.
- Thorpe LM, et al. (2017) PI3K-p110 α mediates the oncogenic activity induced by loss of the novel tumor suppressor PI3K-p85 α . *Proc Natl Acad Sci USA* 114:7095–7100.
- Zhang Z, et al. (2016) Insulin resistance and diabetes caused by genetic or diet-induced KBTBD2 deficiency in mice. *Proc Natl Acad Sci USA* 113:E6418–E6426.
- Geering B, Cutillas PR, Nock G, Gharbi SI, Vanhaesebroeck B (2007) Class IA phosphoinositide 3-kinases are obligate p85-p110 heterodimers. *Proc Natl Acad Sci USA* 104:7809–7814.
- Mechold U, Gilbert C, Ogryzko V (2005) Codon optimization of the BirA enzyme gene leads to higher expression and an improved efficiency of biotinylation of target proteins in mammalian cells. *J Biotechnol* 116:245–249.
- Beckett D, Kovaleva E, Schatz PJ (1999) A minimal peptide substrate in biotin holoenzyme synthetase-catalyzed biotinylation. *Protein Sci* 8:921–929.
- Foukas LC, et al. (2006) Critical role for the p110alpha phosphoinositide-3-OH kinase in growth and metabolic regulation. *Nature* 441:366–370.
- Vanhaesebroeck B, Ali K, Bilancio A, Geering B, Foukas LC (2005) Signalling by PI3K isoforms: Insights from gene-targeted mice. *Trends Biochem Sci* 30:194–204.
- Zhao JJ, et al. (2006) The p110alpha isoform of PI3K is essential for proper growth factor signaling and oncogenic transformation. *Proc Natl Acad Sci USA* 103:16296–16300.
- Guillermet-Guibert J, et al. (2008) The p110beta isoform of phosphoinositide 3-kinase signals downstream of G protein-coupled receptors and is functionally redundant with p110gamma. *Proc Natl Acad Sci USA* 105:8292–8297.
- Okkenhaug K, et al. (2002) Impaired B and T cell antigen receptor signaling in p110delta PI 3-kinase mutant mice. *Science* 297:1031–1034.
- Fruman DA, et al. (1999) Impaired B cell development and proliferation in absence of phosphoinositide 3-kinase p85alpha. *Science* 283:393–397.
- Burke JE, Williams RL (2015) Synergy in activating class I PI3Ks. *Trends Biochem Sci* 40:88–100.
- Jimenez C, Hernandez C, Pimentel B, Carrera AC (2002) The p85 regulatory subunit controls sequential activation of phosphoinositide 3-kinase by Tyr kinases and Ras. *J Biol Chem* 277:41556–41562.
- Clark J, et al. (2011) Quantification of PtdInsP3 molecular species in cells and tissues by mass spectrometry. *Nat Methods* 8:267–272.